ELSEVIER

Chemical Physics 247 (1999) 133–139

Chemical Physics

www.elsevier.nl/locate/chemphys

Manipulating the biochemical nanoenvironment around single molecules contained within vesicles

Daniel T. Chiu [a,1], Clyde F. Wilson [a], Anders Karlsson [b], Anna Danielsson [b], Anders Lundqvist [b], Anette Strömberg [b], Frida Ryttsén [b], Maximilian Davidson [b], Sture Nordholm [b], Owe Orwar [b], Richard N. Zare [b,*]

[a] *Department of Chemistry, Stanford University, Stanford, CA 94305-5080, USA*
[b] *Department of Chemistry, Göteborg University, Göteborg, SE-41296, Sweden*

Received 4 January 1999

Abstract

A method to study single-molecule reactions confined in a biomimetic container is described. The technique combines rapid vesicle preparation, optical trapping and fluorescence confocal microscopy for performing simultaneous single-vesicle trapping and single-molecule detection experiments. The collisional environment between a single enzyme and substrate inside a vesicle is characterized by a Brownian dynamics Monte Carlo simulation.

Keywords: Biochemical nanoenvironment; Single molecules; Vesicles

1. Introduction

Recent advances in optics and microscopy have permitted the optical detection and study of single molecules under biologically relevant conditions [1–4]. The dynamics of single biological molecules, for example, have been investigated in detail [5–11], and the conformational motions of single DNA molecules were recorded and analyzed [12]. Striking visual images of single molecules were also obtained under various conditions, such as on surfaces using near-field or confocal optics [13,14], in solution with wide-field illumination [15], and on lipid films [16]. Motions of single molecules in solution were also studied in detail [17–23]. Many interesting and surprising results have been obtained with such single-molecule techniques. For example, optical switching properties of single, green fluorescent protein molecules were reported, which might have useful technological applications [24]. In addition to detecting single molecules by single-photon-excited fluorescence, other complementary optical techniques have also been demonstrated for the study of single molecules, including the use of multiphoton excitation [25,26] and surface-enhanced Raman scattering [27,28].

Not only can single molecules be optically detected, individual biological macromolecules can also

* Corresponding author. Fax: +1-650-725-0259; E-mail: rnz@leland.stanford.edu

[1] Present address: Department of Chemistry and Chemical Biology, Harvard University, 12 Oxford Street, Cambridge, MA 02138, USA.

0301-0104/99/$ - see front matter
PII: S0301-0104(99)00154-8

be manipulated by optical means. For instance, the direct optical trapping of a single DNA molecule without the use of a handle has been demonstrated [29,30]. With the help of microbead handles, polymer physics of single DNA molecules have been studied in detail [31]. In combination with optical interferometry or a quad cell, this optical trapping technique was also used to measure the force generated by single biological macromolecules with high accuracy [32,33]. Interesting results obtained through these force measurements have provided important insights into the workings of mechanoproteins and biomotors.

Although ultrasensitive techniques exist to manipulate and detect single molecules, few methods exist to control and manipulate the nanoenvironment surrounding a single molecule. By confining single molecules to such a controlled nanoenvironment, the dynamics of single-molecule reactions can be probed and the observed details can be more meaningfully interpreted. By systematically varying the nanoenvironement, additional insight into single-molecule dynamics might be obtained. Most advances in the area of single-molecule detection concern the ability to do more detailed correlated measurements by increasing the detection sensitivity. In this paper, we describe the use of vesicles to spatially confine biochemical reactions inside a biomimetic container. We also performed simulations to characterize the reaction conditions within such an ultrasmall, confined nanoenvironment. Because the reaction conditions inside cells are heavily compartmentalized, the reported technique and simulation should be of particular importance in understanding biochemical reactions in cells and subcellular organelles.

2. Computational details

For estimation of the collision frequency inside a vesicle, a substrate (S) with radius r_S and an enzyme (E) with radius r_E were treated as hard spheres enclosed in a spherical container with hard walls and of radius r_V. A collision between S and E occurs when they are separated by a minimal distance R_{SE}, such that $R_{SE} = r_S + r_E$. This condition creates an excluded volume around each molecule with respect to the other. Therefore, the collision frequency between S and E can be estimated without explicitly accounting for the solvent by calculating the influx of particles into the excluded volume, given by:

$$\omega_{SE} = \left(r_{SE}^2/V\right)\left(8\pi k_B T/\mu\right)^{1/2}, \quad (1)$$

where ω_{SE} is the collision frequency, V is the vesicle volume, k_B is the Boltzmann constant, T is the temperature (Kelvin) and μ is the reduced mass. Using similar arguments, we can obtain the substrate–wall and enzyme–wall collision frequencies (ω_{SW} and ω_{EW}, respectively):

$$\omega_{SW} = (3/r_V)\left(k_B T/2\pi m_S\right)^{1/2} \quad (2)$$

and

$$\omega_{EW} = (3/r_V)\left(k_B T/2\pi m_E\right)^{1/2}. \quad (3)$$

A simplified Brownian diffusion dynamics model accounts for the influence of the solvent. A rough estimate of the radius of the molecules was obtained by using the Stokes–Einstein equation, where the diffusion coefficient (D) does not account for any effects due to charge. This approximation applies to large molecules like enzymes, but might not be accurate for substrates [34]. Small molecules and ions are mostly hydrated; hence, the observed diffusion coefficients are those of the solvated molecules or ions. In our model, the diffusion coefficients were estimated from molecules of approximately the same molecular weight. We took $D = 7 \times 10^{-11}$ m^2/s for alkaline phosphatase (AP) and $D = 4.4 \times 10^{-10}$ m^2/s for fluorescein diphosphate. We note that D also depends on other variables, including molecular volume, molecular geometry, and molecule–medium interactions.

Several algorithms have been used to describe Brownian-type motions [35–37]. We used a simplified model in which we assume the velocities of the molecules to be constant over the small time steps taken. By changing the timesteps and the constant velocities, a given diffusion coefficient can be modeled. The trajectories of the molecules can be followed and the average displacement at a certain time can be calculated and used to obtain the diffusion constant by the relationship $D = \lim_{t\to\infty} \langle x^2(t)\rangle/2t$ [38].

In our simple model, we used a random displacement with a Monte-Carlo step in which the random number generated is uniformly distributed between

−1 and 1. In this way, we were able to get an estimate of the velocities and the timesteps to be used in the simulation. Because $\langle x_n^2 \rangle = 2Dndt$ ($t = ndt$), which gives $D = \langle x_n^2 \rangle / (2ndt)$, the diffusion coefficient can be estimated from the model. We allow the substrate and the enzyme to have a maximum random displacement of almost equal size. In this way, the solvent had a greater effect on the substrate because the substrate made four random displacements while the enzyme made only one.

3. Experimental details

3.1. Optical setup

To initiate and probe chemical reactions inside individual vesicles, dual near-IR and visible laser beams were used to perform simultaneous optical trapping [29,39] and fluorescence confocal microscopy [22,23] (Fig. 1). Briefly, the optical trap was formed by first sending the output (992 nm) of a MOPA diode laser (SDL, San Jose, CA, USA) through a spatial filter. The beam was then reflected by a polychroic beamsplitter (Chroma Technology, Brattleboro, VT, USA) and focused by a high numerical aperture objective (N.A. 1.3). The fluorescence confocal microscopy setup consists of sending the 488-nm line of an argon ion laser (Spectra Physics, Mountain View, CA, USA) through a telescope, and then reflected by the polychroic beamsplitter into the high N.A. objective. The tight foci of the 992- and 488-nm laser beams were laterally superimposed on each other by independently controlling the angles the two beams entered the objective, and longitudinally superimposed by adjusting the telescope. The emitted fluorescence photons were collected by the objective, transmitted through the polychroic beamsplitter, passed through a 50-μm pinhole, and detected by a single-photon-avalanche diode detector (EG&G Optoelectronics, Quebec, Canada). The signal was collected by a multichannel scaler (EG&G Ortec, Oak Ridge, TN, USA) and displayed on a computer.

3.2. Preparation of vesicles

The rapid preparation of large liposomes was described elsewhere [40]. Briefly, a flask with 3 μl

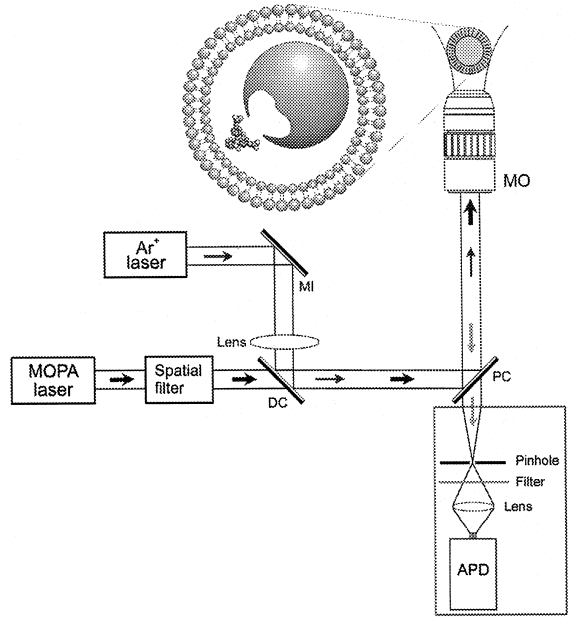

Fig. 1. Schematic diagram of the experimental setup. The vesicle encapsulated enzyme–substrate reaction system is trapped and manipulated by a MOPA diode laser. The 488-nm line of an Ar+ ion laser is then used to excite the fluorescent product (fluorescein) of the enzyme–substrate reaction. The resulting fluorescence photons are collected, sent through a pinhole, and focused onto a single-photon-avalanche diode detector. The size of the vesicle is matched to the laser focus for optimal detection. The light-beam representation in the box is different than in the rest of the schematic. The vesicle containing enzyme and substrate is enlarged and drawn in arbitrary scale. Abbreviations: MI = mirror, DC = dichroic mirror, MO = microscope objective, PC = polychroic mirror, APD = avalanche photodiode.

0.1 M L-α-phosphatidylcholine (PC) (Sigma, St. Louis, MO, USA) in chloroform, 110 μl chloroform, 30 μl methanol, and 1 ml of buffer solution containing enzyme (AP from Sigma) or substrate (fluorescein diphosphate from Molecular Probes, Europe, Leiden, Netherlands) or both, was rota-evaporated under reduced pressure at 40–42°C for 2 min. After evaporation, organic solvents were removed. The remaining buffer solution contained liposomes that ranged from submicrons to approximately 100 μm in diameter. To prepare vesicles less than 100 nm in diameter, 200 μl of PC was dried in a rota-evaporator for 1 h, suspended in 1 ml of potassium phosphate buffer (5 mM Tris–SO_4, 120 mM KPi, 1 mM $MgSO_4$, 0.5 mM EDTA, 1% glycerol, pH 7.5), and then solubilized by addition of 90 μl 20% sodium

cholate 250 μl of 3 M NaCl, 924 μl of 20 mM CHAPS in 50 mM sodium phosphate buffer. For preparation of small unilamellar vesicles, 200 μl of the above lipid/detergent/salt mixture was added to a pretreated spin column (equilibrated with buffer containing analytes and spun to remove void volume), and centrifuged at low speed to elute the vesicles. The vesicle solution was then run through a size-exclusion column to remove the extravesicular analytes.

4. Results and discussion

From the Brownian dynamics Monte-Carlo simulations, we calculated the number of collisions between enzyme and substrate and between the contained molecules and the vesicle wall. Fig. 2A and B show the diffusive paths of the vesicle-confined substrate and the enzyme, respectively. Because of the smaller size and faster diffusive movement of the substrate, it is able to sample more space inside the vesicle, which is reflected in the dense, more crowded trajectories. Fig. 2C traces the substrate–wall collisions during a 60-μs simulation.

Fig. 3 is a plot of the collision frequency as a function of vesicle size. Inside a 170-nm diameter vesicle, a single enzyme and a single substrate collide at a rate of 300 kHz. The enzyme–wall collision frequency for this vesicle is above 50 MHz, over 150 times more frequent than the enzyme–substrate interactions; the substrate–wall collision rate is 200 MHz, almost 1000 times the enzyme–substrate collison frequency. This fact implies that surface interactions can have significant or even dominant effects over the rate and mechanism of biochemical reactions. This simulated collison environment inside a vesicle assumed a perfect spherical reflective boundary for the wall (zero residence time), and did not account for any charge or hydrophobic interactions

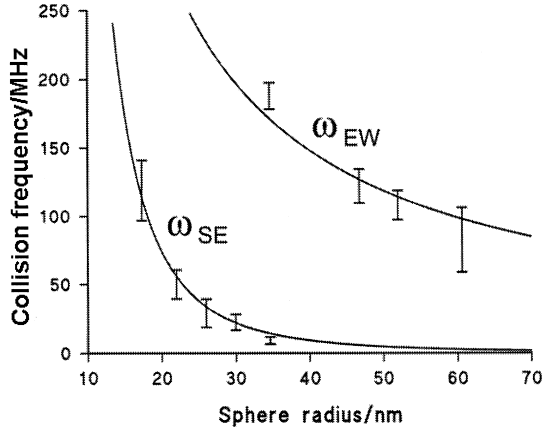

Fig. 3. A plot showing collision frequency vs. vesicle radius. ω_{SE} is the substrate–enzyme collision frequency (40×10^6 steps, each at 1.5 ps), and ω_{EW} is the enzyme–wall collision frequency (10×10^6 steps, each at 6 ps). The functions were fitted to $y = kx^{-r}$, where $r = -3$ for ω_{SE} (correlation coefficient = 0.997) and -1 for ω_{EW} (correlation coefficient = 0.999) to demonstrate the volume and radius dependence, respectively.

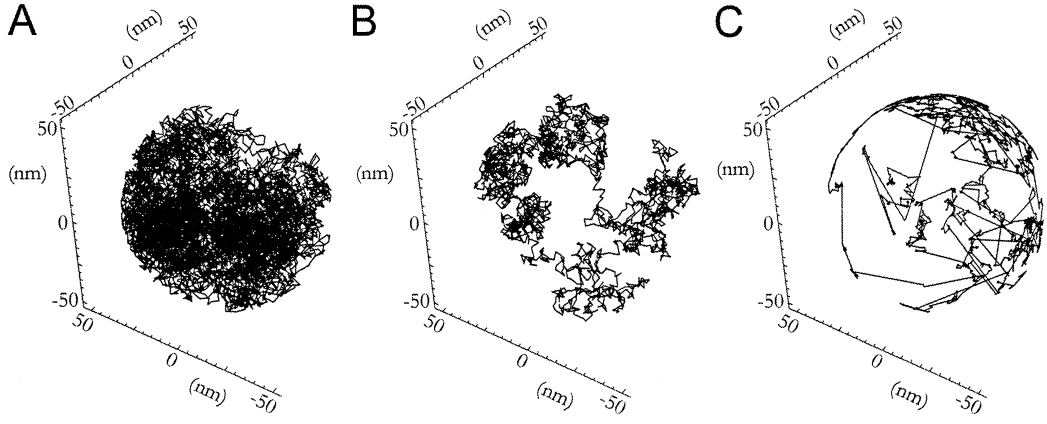

Fig. 2. Trajectories of a single substrate (A) and enzyme (B) inside a 104-nm diameter sphere modelled using a Brownian dynamics Monte-Carlo simulation. The substrate was followed for 10^4 steps with each step at 10 ns, and the enzyme was followed for 2.5×10^3 steps with each step at 40 ns. (C) A trace showing collisions between a single substrate and the spherical wall (same simulation conditions as in (A) and (B), substrate was followed for 40×10^6 steps, each step at 1.5 ps).

between the wall and the contained molecules. If these effects were included, molecules inside biocompartments can be significantly biased to reside near (or away from) the wall of the biocompartment. Indeed, if both molecules spend sufficient time near the wall, most reactions might occur at or near the wall because collisions between two-dimensionally diffusing molecules are more likely than from three-dimensional diffusion. The membrane composition of cells is precisely regulated; phosphatidyl serine (negatively charged), for example, is partitioned exclusively to the inner leaflet of the bilayer. In combination with the small size of subcellular compartments (tens of nanometers in diameter), these precisely regulated surfaces are expected to have important influences over the rate of biochemical reactions.

Fig. 4 shows the time when collisions between enzyme and substrate occur. During this simulation (60-μs run time), approximately 1500 substrate–enzyme collisions took place, owing to the small size of the vesicle (60 nm). It is evident from Fig. 4 that collisions in this vesicle occur in clusters. This clustering effect arose because once a collision happened, the two molecules remain for some time in the neighborhood of each other. Hence, subsequent collisions are more likely. If a reaction requires multiple collisions for completion, this clustering behavior might result in a non-Poissonian rate distribution, because Poisson statistic assumes temporally uncorrelated random events. A reaction that occurs after only one or a few collisions (diffusion-limited reactions) should still obey Poisson statistics, because the occurrence of the clusters appears to be uncorrelated in time.

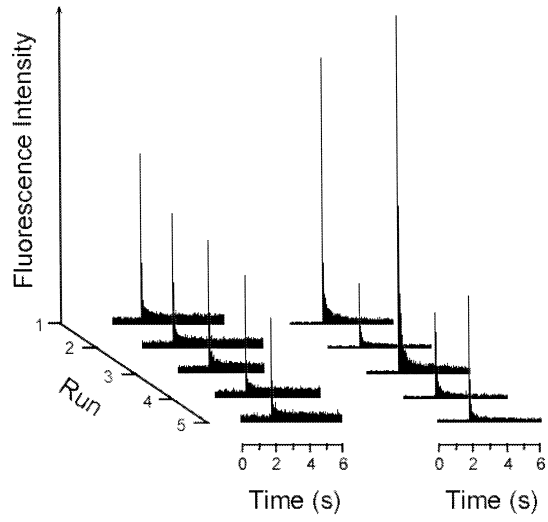

Fig. 5. Fluorescence intensity vs. time as a measure of AP catalytic activity inside an optically trapped vesicle containing AP and 0.75 mM fluorescein diphosphate. At 60-s intervals, the amount of fluorescent products accumulated was simultaneously probed and bleached at 488 nm. The bleaching resets the reaction clock for each run. The vesicle in the left panel had a radius of 1.5 μm, and the vesicle in the right panel had a radius of 500 nm.

The ability to follow reaction dynamics at the single-molecule level offers the special opportunity to study the effects of such molecule–wall interactions. To monitor optically the behaviors and reactions of single biomolecules evolving in time, the molecule must be localized within the ultrasmall laser probe volume. Although methods exist to im-

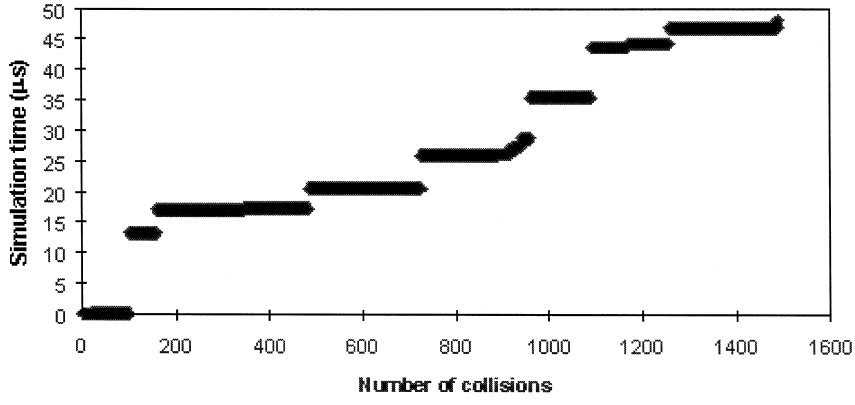

Fig. 4. Occurrence of substrate–enzyme collisions during a 60-μs simulation. The vesicle diameter used was 60 nm.

mobilize and study the kinetics of single molecules, these techniques might introduce unwanted perturbations into the measurements. Consequently, it is difficult to infer the true in vivo biological activities of these biomolecules from in vitro experiments that do not confine these biomolecules in containers that mimic their in vivo environment. Fig. 5 shows the turnover of substrates into products by enzyme molecules contained in a phosphatidylcholine vesicle. Based on the low enzyme concentration used, only one to a few enzymes should be present in each vesicle. The actual number density, however, is likely to vary significantly between vesicles and would depend strongly on the size and encapsulation efficiency of each vesicle. The trapping near-IR beam serves to immobilize the vesicle within the volume (1 fl) of the probe beam (Fig. 1). The small size of the vesicles provides a good size match with the confocal detection volume. Therefore, the trapped vesicle serves both to immobilize the molecules of interest and to approximate in first-order the in vivo nanoenvironment inside a cell or cellular compartment. In the left panel of Fig. 5, the amount of products formed is quite homogeneous over time, which is in sharp contrast to the product formation rate shown in the right panel. The nature of this difference is unclear at present. By systematically varying the membrane composition and reaction condition, however, a detailed understanding of this difference is expected to be obtained. A recently developed technique to initiate and control chemical reactions in individual biomimetic containers is of particular relevance in the study of such single-molecule dynamics within vesicles [41].

Experiments on single-enzyme kinetics have provided exciting results. For example, the turnover rate of single enzymes was studied by localizing the enzyme in agarose gel [5], microwells [7] and glass capillaries [6,8]. Interesting variations between individual enzymes have been observed [5–8]. But are these differences caused by variations in local nanoenvironments or by the different ways in which these enzymes were attached? Do they represent true biological variations? These types of questions can only be addressed by studying the reaction under conditions that approximate the intimate presence of a membrane wall. Indeed, even traditional measurements of enzymatic activities in bulk solutions might not truly represent the reaction conditions inside the highly compartmentalized cell, where strong interactions with bilayer membranes exist.

Acknowledgements

We thank Susan Orwar for graphics work. C.F.W. acknowledges support from the Stanford Graduate Fellowship. This work is supported by the U.S. National Institute on Drug Abuse (DA09873), the Swedish Foundation for Strategic Research, and by the Swedish Research Council for Engineering Sciences.

References

[1] S. Nie, R.N. Zare, Annu. Rev. Biophys. Biomol. Struct. 26 (1997) 567.
[2] X.S. Xie, J.K. Trautman, Annu. Rev. Phys. Chem. 59 (1998) 441.
[3] T. Basch, W.E. Moerner, M. Orrit, U.P. Wild (Eds.), Single Molecule Optical Detection, Imaging and Spectroscopy, VCH, Weinheim, 1997.
[4] D.T. Chiu, R.N. Zare, Chem. Eur. J. 3 (1997) 335.
[5] H.P. Lu, L. Xun, X.S. Xie, Science 282 (1998) 1877.
[6] Q. Xue, E. Yeung, Nature 373 (1995) 681.
[7] W. Tan, E.S. Yeung, Anal. Chem. 69 (1997) 4242.
[8] D.B. Craig, E.A. Arriaga, J.C.Y. Wong, H. Lu, N.J. Dovichi, J. Am. Chem. Soc. 118 (1996) 5245.
[9] T. Funatsu, Y. Harada, M. Tokunaga, K. Saito, T. Yanagida, Nature 374 (1995) 555.
[10] A. Ishijima, H. Kojima, T. Funatsu, M. Tokunaga, H. Higuchi, H. Tanaka, T. Yanagida, Cell 92 (1998) 161.
[11] H. Noji, R. Yasuda, M. Yoshida, K. Kinosita, Nature 386 (1997) 299.
[12] S. Wennmalm, L. Edman, R. Rigler, Proc. Natl. Acad. Sci. U.S.A. 94 (1997) 10641.
[13] J.K. Trautman, J.J. Macklin, L.E. Brus, E. Betzig, Nature 369 (1994) 40.
[14] T. Ha, J. Glass, T. Enderle, D.S. Chemla, S. Weiss, Phys. Rev. Lett. 80 (1998) 2093.
[15] X.H.N. Xu, E.S. Yeung, Science 281 (1998) 5383.
[16] T. Schmidt, G.J. Schutz, W. Baumgartner, H.J. Gruber, H. Schindler, Proc. Natl. Acad. Sci. U.S.A. 93 (1996) 2926.
[17] C. Eggeling, J.R. Fries, L. Brand, R. Gunther, C.A. Seidel, Proc. Natl. Acad. Sci. U.S.A. 95 (1998) 1556.
[18] M.A. Osborne, S. Balasubramanian, W.S. Furey, D. Klenerman, J. Phys. Chem. B 102 (1998) 3160.
[19] A. Van Orden, N.P. Machara, P.M. Goodwin, R.A. Keller, Anal. Chem. 70 (1998) 1444.
[20] M. Eigen, R. Rigler, Proc. Natl. Acad. Sci. U.S.A. 91 (1994) 5740.
[21] R. Rigler, U. Mets, J. Widengren, K. Kask, Eur. Biophys. J. 22 (1993) 169.

[22] S. Nie, D.T. Chiu, R.N. Zare, Science 266 (1994) 1018.
[23] S. Nie, D.T. Chiu, R.N. Zare, Anal. Chem. 67 (1995) 2849.
[24] R.M. Dickson, A.B. Cubitt, R.Y. Tsien, W.E. Moerner, Nature 388 (1997) 355.
[25] J. Mertz, C. Xu, W.W. Webb, Opt. Lett. 20 (1995) 2532.
[26] M.A. Bopp, Y. Jia, G. Haran, E.A. Morlino, R.M. Hochstrasser, Appl. Phys. Lett. 73 (1998) 7.
[27] S. Nie, S.R. Emory, Science 275 (1997) 1102.
[28] K. Kneipp, Y. Wang, H. Kneipp, L.T. Perelman, I. Itzkan, R. Dasari, M.S. Feld, Phys. Rev. Lett. 78 (1997) 1667.
[29] D.T. Chiu, R.N. Zare, J. Am. Chem. Soc. 118 (1996) 6512.
[30] S. Katsura, K. Hirano, Y. Matsuzawa, K. Yoshikawal, A. Mizuno, Nucleic Acids Res. 26 (1998) 4943.
[31] T.T. Perkins, D.E. Smith, R.G. Larson, S. Chu, Science 268 (1995) 83.
[32] H. Yin, M.D. Wang, K. Svoboda, R. Landick, S.M. Block, J. Gelles, Science 270 (1995) 1653.
[33] S.B. Smith, Y. Cui, C. Bustamante, Science 271 (1996) 795.
[34] D.L. Ermak, J. Chem. Phys. 62 (1975) 4189.
[35] M.P. Allen, Mol. Phys. 40 (1980) 1073.
[36] M.P. Allen, Mol. Phys. 47 (1982) 599.
[37] W.F. van Gunsteren, H.J.C. Berendsen, Mol. Phys. 45 (1982) 637.
[38] P. Turq, F. Lantalme, H.L. Friedman, J. Chem. Phys. 66 (1977) 3039.
[39] D.T. Chiu, A. Hsiao, A. Gaggar, R.A. Garza-Lopez, O. Orwar, R.N. Zare, Anal. Chem. 69 (1997) 1801.
[40] A. Moscho, O. Orwar, D.T. Chiu, B.P. Modi, R.N. Zare, Proc. Natl. Acad. Sci. U.S.A. 93 (1996) 11443.
[41] D.T. Chiu, C.F. Wilson, F. Ryttsén, A. Strömberg, C. Farre, A. Karlsson, S. Nordholm, A. Gaggar, B.P. Modi, A. Moscho, R.A. Garza-Lopéz, O. Orwar, R.N. Zare, Science 283 (1999) 1892.